Phytochemistry 80 (2012) 137–147

Contents lists available at SciVerse ScienceDirect

Phytochemistry

journal homepage: www.elsevier.com/locate/phytochem

Sesquiterpenes from the roots of *Illicium dunnianum*

Jian Bai, Hui Chen, Zhen-Feng Fang, Shi-Shan Yu *, Wen-Jie Wang, Yang Liu, Shuang-Gang Ma, Yong Li, Jing Qu, Song Xu, Jun-Hong Liu, Fen Zhao, Nan Zhao

State Key Laboratory of Bioactive Substance and Function of Natural Medicines, Institute of Materia Medica, Chinese Academy of Medical Sciences and Peking Union Medical College, Beijing 100050, People's Republic of China

ARTICLE INFO

Article history:
Received 18 August 2011
Received in revised form 27 February 2012
Available online 11 June 2012

Keywords:
Illicium dunnianum
Illiciaceae
allo-Cedrane sesquiterpenes
seco-Prezizaane-type sesquiterpenes
Monocyclofarnesane sesquiterpenes
Polymorphonuclear leukocytes
Cytotoxicity

ABSTRACT

Six *allo*-cedrane sesquiterpenes, four *seco*-prezizaane-type sesquiterpenes, two monocyclofarnesane sesquiterpenes, together with four known sesquiterpenes, were isolated from the roots of *Illicium dunnianum*. The structures were elucidated by spectroscopic methods including 1D and 2D NMR. The absolute configuration of **10** was determined by a CD experiment. Compounds **11** and **13** showed potent activities against the release of β-glucuronidase in rat polymorphonuclear leukocytes induced by platelet-activating factor *in vitro*, with IC_{50} values of 2.10 ± 0.40 and 1.93 ± 0.57 μM, respectively. All compounds were evaluated for cytotoxicities against five human cancer cell lines (A549, Bel-7402, BGC-823, HCT-8, and A2780) in the MTT assay, but none of them exhibited activity at concentrations tested (10^{-5}–10^{-7} M).

1. Introduction

Species of the genus *Illicium* L. (Illiciaceae) are known to be characterized by a variety of structurally unique sesquiterpenes such as *seco*-prezizaane-type (Huang et al., 2002; Schmidt, 1999; Yamada et al., 1968), anislactone (Huang et al., 2001b; Kouno et al., 1989c), and *allo*-cedrane sesquiterpenes (Schmidt et al., 2001), some of which were found to exhibit intriguing neurotrophic activities (Huang et al., 2001a; Kubo et al., 2009; Yokoyama et al., 2002). *Illicium dunnianum* is a toxic shrub distributed in Southern China and used as a folk medicine for relieving pain and treating rheumatism (Zhang, 1989). In previous papers, *seco*-prezizaane-type sesquiterpenes with anti-inflammatory activities (Tang et al., 2009), prenylated C_6–C_3 compounds with cytotoxicities (Ma et al., 2011), and neolignan glycosides (Tang et al., 2007) were isolated from *I. oligandrum*. As part of our ongoing search for structurally unique and biologically interesting *Illicium* sesquiterpenes, the chemical constituents of the roots of *I. dunnianum* were investigated, which resulted in the isolation of six new *allo*-cedrane sesquiterpenes possessing a tetracyclic ketal structure, tashironin B (**1**), tashironin C (**2**), 2α-hydroxytashironin (**3**), 2α-acetoxytashironin (**4**), 2α-hydroxytashironin A (**5**), and 2α-acetoxytashironin A (**6**), four new *seco*-prezizaane-type sesquiterpenes, dunnianolide A–D (**7**–**10**), two new monocyclofarnesane sesquiterpenes, 8′-oxo-6-hydroxy-dihydrophaseic acid (**11**) and 6-hydroxy-dihydrophaseic acid (**12**), together with four known sesquiterpenes, tashironin (**13**) (Fukuyama et al., 1995), tashironin A (**14**) (Song et al., 2007), 14-*O*-benzoylfloridanolide (**15**) (Huang et al., 2000b), and neoanisatin (**16**) (Yamada et al., 1968) (Fig. 1).

In this paper, the isolation and structure elucidation of these new compounds are described. The activities against the release of β-glucuronidase in rat polymorphonuclear leukocytes (PMNs) induced by platelet-activating factor (PAF) and cytotoxicities of compounds **1**–**16** are also assayed.

2. Results and discussion

The dry and powdered roots of *I. dunnianum* were successively extracted with EtOH–H_2O (95:5, v/v) and EtOH–H_2O (70:30, v/v). The total EtOH extract was absorbed by diatomite, and then successively extracted with petroleum ether (60–90 °C), $CHCl_3$, EtOAc, and MeOH. The $CHCl_3$ and EtOAc extracts were subjected to column chromatography on silica gel, Sephadex LH-20, ODS, and preparative reversed-phase HPLC, respectively, to afford compounds **1**–**16**.

Compound **1** was isolated as a colorless amorphous solid, and its molecular formula was deduced to be $C_{23}H_{28}O_6$ by ESIMS ions at *m*/*z* 401 $[M+H]^+$, 423 $[M+Na]^+$, 439 $[M+K]^+$, 399 $[M-H]^-$, 435 $[M+Cl]^-$ and by a positive HRESIMS ion at *m*/*z* 423.1784 $[M+Na]^+$ (calcd. for 423.1778), which was supported by ^{13}C NMR and DEPT spectroscopic data. The IR spectrum indicated the presence of hydroxy (3485 cm^{-1}), carbonyl (1713 cm^{-1}), and phenyl (1612 and

* Corresponding author. Tel.: +86 10 63165326; fax: +86 10 63017757.
E-mail address: yushishan@imm.ac.cn (S.-S. Yu).

0031-9422/$ - see front matter © 2012 Elsevier Ltd. All rights reserved.
http://dx.doi.org/10.1016/j.phytochem.2012.05.015

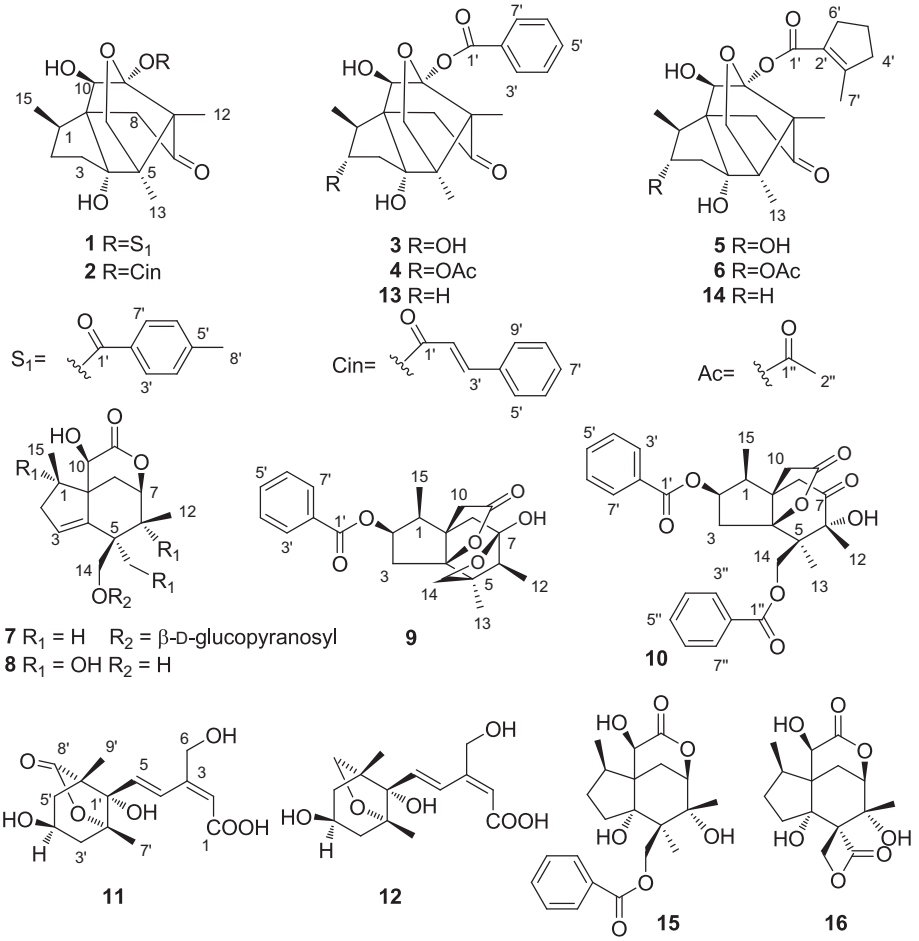

Fig. 1. Chemical structures of compounds **1**–**16**.

1458 cm^{-1}) groups. The ^1H and ^{13}C NMR spectroscopic data (Tables 1 and 2) showed the presence of a *p*-methyl benzoyl group [δ_H 2.41 (3H, s, H_3-8′), 7.86 (2H, d, *J* = 8.0 Hz, H-3′, 7′), 7.22 (2H, d, *J* = 8.0 Hz, H-4′, 6′); δ_C 165.6 (C-1′)]. In addition to the *p*-methyl benzoyl group, the ^1H NMR spectrum of **1** showed signals due to two tertiary methyls [δ_H 1.05 (3H, s, H_3-13) and 1.23 (3H, s, H_3-12)], a secondary methyl [δ_H 1.20 (3H, d, *J* = 7.0 Hz, H_3-15)], an isolated methylene [δ_H 2.14 and 2.60 (each d, *J* = 18.5 Hz, H-8)], and an oxygen-bearing isolated methylene [δ_H 3.85 and 4.21 (each d, *J* = 9.0 Hz, H-14)]. Moreover, the ^1H–^1H COSY spectrum verified the presence of a CH_3(15)–CH(1)–CH_2(2)–CH_2(3) moiety (Fig. 2). The ^{13}C NMR and DEPT spectra of **1** displayed an oxygenated methine carbon at δ_C 76.3 (C-10) and six quaternary carbons including a carbonyl carbon at δ_C 210.9 (C-7) and a ketal-type carbon at δ_C 110.0 (C-11). The above features suggested that **1** exhibited a molecular framework similar to 11-*O*-debenzoyltashironin, which was previously isolated form *I. merrillianum* (Huang et al., 2001a). Furthermore, by comparing the ^{13}C NMR spectroscopic data of **1** with those of 11-*O*-debenzoyltashironin, it was observed that signal for C-11 in **1** was down-shifted to δ_C 110.0 from δ_C 106.4 in 11-*O*-debenzoyltashironin. This indicated that the *p*-methyl benzoxy group was connected to C-11, which was further confirmed by NOESY correlation (Fig. 3) between H_3-12 (δ_H 1.23) and the aromatic H-3′ and/or H-7′ (δ_H 7.86). Extensive HMBC and COSY correlations as shown in Fig. 2 confirmed this structure. The relative configuration of **1** was determined based on a NOESY experiment. NOESY correlations of H-10 to both of H_3-15 and H-8β, of H-14a to H-3β, and of H_3-13 to H_3-12 were observed to establish the relative configuration as shown in Fig. 3. Thus, the structure of **1** was determined as shown in Fig. 1 and designated as tashironin B (**1**).

Compound **2** was obtained as a colorless amorphous solid. Its molecular formula was established as $C_{24}H_{28}O_6$ by positive HRESIMS (*m*/*z* 435.1788 $[M+Na]^+$). The ESI mass spectrum exhibited a peak (*m*/*z* 131, $[C_8H_7CO]^+$) attributable to the presence of a cinnamoyl group. This was confirmed by analysis of the ^1H and ^{13}C NMR spectroscopic data (Tables 1 and 2), which included signals of five aromatic protons at δ_H 7.51 (2H, dd, *J* = 7.5, 2.0 Hz, H-5′, 9′) and 7.38–7.41 (3H, H-6′, 7′, 8′), two olefinic protons at δ_H 6.38 (1H, d, *J* = 16.0 Hz, H-2′) and 7.69 (1H, d, *J* = 16.0 Hz, H-3′), six aromatic carbons at δ_C 133.8 (C-4′), 128.3 (C-5′, 9′), 129.0 (C-6′, 8′), and 130.9 (C-7′), two olefinic carbons at δ_C 116.8 (C-2′) and 147.1 (C-3′), and a carbonyl carbon at δ_C 165.9 (C-1′). The geometry of the disubstituted double bond of the cinnamoyl moiety was determined as *E* by the large vicinal coupling constant value (16.0 Hz) of the olefinic proton between H-2′ (δ_H 6.38) and H-3′ (δ_H 7.69). The NMR spectroscopic data of **2** closely resembled those of 11-*O*-debenzoyltashironin (Huang et al., 2001a), except for the presence of an additional cinnamoyl group. The resonance for C-11 was shifted downfield from δ_C 106.4 in 11-*O*-debenzoyltashironin to δ_C 110.0 in **2**, which suggested that the cinnamoyl group was esterified at C-11. The relative configuration of **2** was the same as that of **1** according to NOESY correlations. Therefore, the structure of **2** was assigned as shown in Fig. 1 and named tashironin C (**2**).

Compound **3** was assigned the molecular formula $C_{22}H_{26}O_7$ by positive HRESIMS (*m*/*z* 425.1587 $[M+Na]^+$). Comparison of the

Table 1
^{13}C NMR spectroscopic data for compounds **1**–**10** (125 MHz for **1**–**10**).[a]

Position	1	2	3	4	5	6	7	8	9	10
1	38.7	38.7	49.7	45.1	49.7	45.1	46.3	81.6	53.2	49.3
2	31.0	31.0	79.9	82.1	79.9	82.2	40.1	49.2	76.8	76.4
3	34.1	34.0	44.2	43.6	44.0	43.6	132.0	133.5	40.9	44.5
4	85.6	85.2	84.3	83.6	84.3	83.6	146.2	137.3	99.6	96.6
5	54.4	54.5	54.0	54.3	53.8	54.1	39.9	50.5	50.7	48.6
6	60.8	60.6	61.0	60.9	60.9	60.8	45.5	75.8	43.5	77.2
7	210.9	210.6	210.0	209.7	210.2	209.9	81.1	86.1	106.1	209.5
8	44.0	44.0	44.0	42.1	44.1	42.0	37.7	25.5	52.3	46.9
9	52.3	52.4	53.7	53.1	53.5	52.9	51.8	56.8	48.9	51.8
10	76.3	76.1	75.5	75.4	75.6	75.5	72.7	73.3	39.7	41.1
11	110.0	110.0	109.9	109.5	109.1	108.8	175.8	176.8	176.1	174.4
12	9.8	9.6	9.8	9.8	9.8	9.7	12.9	22.7	7.9	21.8
13	14.6	14.4	14.4	14.5	14.5	14.6	27.0	62.1	14.1	16.1
14	74.3	74.1	74.4	74.3	74.4	74.3	73.5	65.4	70.8	65.9
15	13.5	13.5	11.5	11.3	11.5	11.3	13.7	22.2	10.0	9.8
1′	165.6	165.9	165.7	165.7	165.1	165.0	103.8		166.2	166.2
2′	126.3	116.8	129.0	129.0	126.3	126.2	73.9		129.8	129.3
3′	130.1	147.1	130.0	130.0	160.5	160.6	77.8		129.5	129.6
4′	129.2	133.8	128.6	128.6	33.3	33.3	71.3		128.4	128.6
5′	144.8	128.3	133.9	134.0	21.2	21.2	77.8		133.2	133.2
6′	129.2	129.0	128.6	128.6	41.0	41.1	62.7		128.4	128.6
7′	130.1	130.9	130.0	130.0	16.7	16.6			129.5	129.6
8′	21.7	129.0								
9′		128.3								
1″				171.2		171.2				166.0
2″				21.4		21.4				133.4
3″, 7″										129.4
4″, 6″										128.7
5″										129.9

[a] Measured in $CDCl_3$ for compounds **1–6**, **9**, and **10**, in acetone-d_6 for compound **7**, and in methanol-d_4 for compound **8**.

Table 2
^{1}H NMR spectroscopic data for compounds **1**–**6** (500 MHz in $CDCl_3$, *J* in Hz).

Position	1	2	3	4	5	6
1	2.27, m	2.27, m	2.14, m	2.42, m	2.12, m	2.39, m
2	Hα 2.09, m	Hα 2.08, m	4.30, dd (8.0, 5.5)	5.15, dd (7.5, 5.5)	4.27, dd (7.5, 5.5)	5.13, dd (7.5, 5.5)
	Hβ 1.75, m	Hβ 1.74, m				
3α	1.50, m	1.50, m	1.58, d (14.5)	1.58, d (15.5)	1.53, d (14.5)	1.55, d (15.0)
3β	2.55, m	2.50, m	2.94, dd (14.5, 8.5)	3.07, dd (15.5, 9.5)	2.93, dd (14.5, 8.5)	3.06, dd (15.0, 9.5)
8α	2.60, d (18.5)	2.59, d (18.5)	2.77, d (18.5)	2.74, d (18.5)	2.72, d (18.5)	2.69, d (18.5)
8β	2.14, d (18.5)	2.16, d (18.5)	2.15, d (18.5)	2.14, d (18.5)	2.09, d (18.5)	2.08, d (18.5)
10	4.07, s	4.05, s	4.00, br s	4.01, s	3.88, br s	3.89, s
12	1.23, s	1.17, s	1.25, s	1.25, s	1.14, s	1.14, s
13	1.05, s	1.03, s	1.06, s	1.05, s	1.02, s	1.01, s
14a	4.21, d (9.0)	4.17, d (9.0)	4.11, d (9.0)	4.14, d (9.0)	4.06, d (9.0)	4.10, d (9.0)
14b	3.85, d (9.0)	3.84, d (9.0)	3.85, d (9.0)	3.86, d (9.0)	3.80, d (9.0)	3.80, d (9.0)
15	1.20, d (7.0)	1.21, d (7.0)	1.30, d (7.0)	1.26, d (7.0)	1.29, d (7.0)	1.25, d (7.0)
2′		6.38, d (16.0)				
3′	7.86, d (8.0)	7.69, d (16.0)	7.97, d (7.5)	7.97, d (7.5)		
4′	7.22, d (8.0)		7.44, t (7.5)	7.44, t (7.5)	2.54, m	2.55, m
5′		7.51, dd (7.5, 2.0)	7.59, t (7.5)	7.59, t (7.5)	1.79, m	1.79, m
6′	7.22, d (8.0)	7.38–7.41, (overlap)	7.44, t (7.5)	7.44, t (7.5)	2.48, m	2.48, m
7′	7.86, d (8.0)	7.38–7.41, (overlap)	7.97, d (7.5)	7.97, d (7.5)	2.07, s	2.07, s
8′	2.41, s	7.38–7.41, (overlap)				
9′		7.51, dd (7.5, 2.0)				
2″				2.06, s		2.05, s
10-OH	3.92, br s		4.02 br s		4.07, br s	

NMR spectroscopic data (Tables 1 and 2) of **3** with those of tashironin (**13**) (Fukuyama et al., 1995) indicated that the structure of **3** was very close to that of **13**, with the exception of the signal assigned to C-2, where the resonance at δ_C 31.1 (C-2) in **13** was shifted downfield to δ_C 79.9 (C-2) in **3**. This indicated that a proton at C-2 in **13** was replaced by a hydroxy group in **3**, which was supported by HMBC correlations between H-2 (δ_H 4.30) and both of C-4 (δ_C 84.3) and C-15 (δ_C 11.5). In addition, the relative configuration of **3** was deduced from NOE correlations. H-2, OH-10, and the C-15 methyl group were all β-oriented, which were confirmed by NOE enhancements of H-2 and H-10 by irradiation of H_3-15. According to the above analysis, the structure of **3** was elucidated as 2α-hydroxytashironin (**3**).

The molecular formula of compound **4** was established as $C_{24}H_{28}O_8$ by positive HRESIMS (*m/z* 467.1687 $[M+Na]^+$). Furthermore, the ^{1}H and ^{13}C NMR spectra (Tables 1 and 2) of **4** showed close resemblance to those of **3**, except for the presence of an additional *O*-acetyl group [δ_C 171.2 (C-1″), δ_H 2.06 (3H, s, H_3-2″)] relative to **3**. It was observed that the signal for H-2 was downfield-shifted from δ_H 4.30 in **3** to δ_H 5.15 in **4**, and H-2 showed

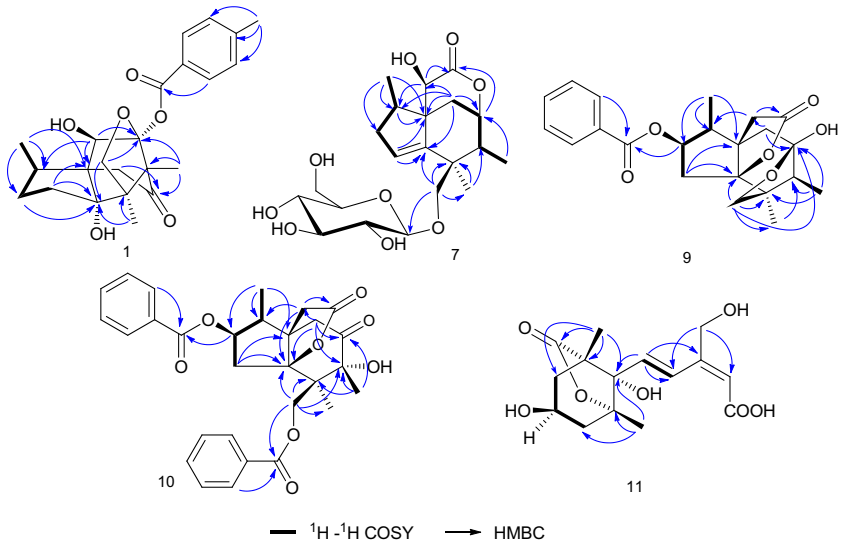

Fig. 2. Key HMBC and ^{1}H–^{1}H COSY correlations of **1**, **7**, **9**, **10**, and **11**.

an HMBC correlation with the carbonyl carbon at δ_C 171.2 (C-1″), which suggested that **4** was the 2-*O*-acetyl derivative of **3**. Moreover, the relative configuration of the C-2 acetoxy group was unambiguously proven by a NOE experiment, which showed interactions from H-2 to both H_3-15 and H-3β, and from H_3-15 to H-10, thereby confirming the α-orientation of the C-2 acetoxy group. Thus, **4** was established as 2α-acetoxytashironin (**4**).

Compound **5** was assigned the molecular formula $C_{22}H_{30}O_7$ by positive HRESIMS (*m*/*z* 429.1861 [M+Na]$^+$). The ^{13}C NMR spectroscopic data (Table 1) of **5** were very similar to tashironin A (**14**) (Song et al., 2007) except that the signal for C-2 at δ_C 31.0 in **14** was shifted downfield to δ_C 79.9 in **5**, which suggested that **5** was the 2-hydroxy derivative of **14**. The location of the hydroxy group at C-2 was further confirmed by the HMBC correlations of H-2 (δ_H 4.27) to C-4 (δ_C 84.3) and C-15 (δ_C 11.5). Additionally, the relative configuration of the C-2 hydroxy group was determined on the basis of NOESY correlations. H_3-15 showed NOESY interactions with H-2 and H-10, indicating the α-orientation of the C-2 hydroxy group. Therefore, **5** was deduced to be 2α-hydroxytashironin A (**5**).

The molecular formula of compound **6** was deduced to be $C_{24}H_{32}O_8$ by positive HRESIMS (*m*/*z* 471.1971 [M+Na]$^+$). The NMR spectroscopic data (Tables 1 and 2) of **6** were closely related to those of **5** except for the presence of an additional *O*-acetyl group and the shift of signal corresponding to H-2 from δ_H 4.27 in **5** to δ_H 5.13 in **6**. In HMBC spectrum, the signal at δ_H 5.13 (H-2) showed a cross-peak with the *O*-acetyl carbonyl carbon resonance at δ_C 171.2 (C-1″), which confirmed that the acetoxy group was connected to C-2. The NOE correlations of **6** were identical to those observed for **5**, indicating that these two compounds had the same relative configuration. Accordingly, the structure of **6** was elucidated as 2α-acetoxytashironin A (**6**).

Compound **7** was obtained as a colorless amorphous solid. Its molecular formula was deduced to be $C_{21}H_{32}O_9$ by positive HRESIMS (*m*/*z* 451.1939 [M+Na]$^+$). The IR absorption bands at 3437 cm^{-1} and 1718 cm^{-1} indicated the presence of hydroxy and carbonyl groups, respectively. In the ^{13}C NMR spectrum, six carbon resonances at δ_C 103.8 (C-1′), 73.9 (C-2′), 77.8 (C-3′), 71.3 (C-4′), 77.8 (C-5′), and 62.7 (C-6′) were readily assigned to be a glycosyl moiety. The hydrolysis of **7** with 2 M HCl–H_2O afforded a glucose, which was confirmed by TLC with an authentic sample of glucose. The large coupling constant (8.0 Hz) of the anomeric proton at δ_H 4.21 (H-1′) indicated that the glucose was in the β-configuration. GC analysis established the d-configuration of the glucose (Hara et al., 1987).

Additionally, the ^{1}H and ^{13}C NMR spectroscopic data (Tables 1 and 3) indicated the presence of a trisubstituted olefinic bond [δ_H 5.94 (1H, dd, *J* = 3.0, 1.5 Hz, H-3); δ_C 132.0 (C-3) and 146.2 (C-4)], a tertiary methyl [δ_H 1.25 (3H, s, H_3-13)], two secondary methyls [δ_H 1.13 (6H, d, *J* = 7.0 Hz, H_3-12, 15)], an oxygen-bearing isolated methylene [δ_H 3.70 and 3.33 (each d, *J* = 9.5 Hz, H-14)], two methylenes [δ_H 2.28 (1H, ddd, *J* = 14.0, 7.0, 3.0 Hz, H-2α), 2.08 (1H, ddd, *J* = 14.0, 9.5, 1.5 Hz, H-2β); δ_H 1.62 (1H, dd, *J* = 13.5, 1.5 Hz, H-8α), 2.34 (1H, dd, *J* = 13.5, 4.5 Hz, H-8β)], and a carbonyl carbon at δ_C 175.8 (C-11). The ^{1}H–^{1}H COSY spectrum showed the presence of a CH_3(15)–CH(1)–CH_2(2)–CH(3) = partial unit (Fig. 2). Except for the glucosyl moiety, the NMR spectroscopic data of **7** were found to be similar to those of 3,4-dehydrofloridanolide (Huang et al., 2000a). However, the signal for H_3-12 at δ_H 1.13 split into a doublet coupled to quartet of a doublet for H-6 at δ_H 1.77. The resonance for C-6 was up-shifted from δ_C 74.0 in 3,4-dehydrofloridanolide to δ_C 45.5 in **7**. These findings indicated that **7** was the 6-deoxy derivative of 3,4-dehydrofloridanolide, which was further confirmed by the presence of a CH_3(12)–CH(6)–CH(7)–CH_2(8) moiety based on a COSY experiment (Fig. 2). Moreover, the AB doublet assignable to H_2-14 were shifted downfield from δ_H 3.09 and 3.34 in 3,4-dehydrofloridanolide to δ_H 3.33 and 3.70 in **7**, suggesting that the glucosyl moiety was linked to C-14. This was supported by an HMBC correlation (Fig. 2) between H-14a (δ_H 3.70) and the anomeric carbon at δ_C 103.8 (C-1′). The NOESY spectrum showed cross-peaks between H_3-15 and H-10, between H_3-12 and H-14a, and between H-6 and both H_3-13 and H-8α, indicating the α-orientation of Me-13 and the β-orientation of Me-15, Me-12, and OH-10 (Fig. 3). Accordingly, the structure of **7** was elucidated as 14-*O*-β-D-glucopyranosyl-6-deoxy-3,4-dehydrofloridanolide, and designated as dunnianolide A (**7**).

The molecular formula of compound **8** was deduced to be $C_{15}H_{22}O_7$ by analysis of positive HRESIMS (*m*/*z* 337.1261 [M+Na]$^+$). The ^{1}H and ^{13}C NMR spectroscopic data of **8** (Tables 1 and 3) were similar to those of 13,14-dihydroxy-3,4-anhydrofloridanolide (Schmidt et al., 2001). The major differences were that signal for H_3-15 (δ_H 1.28) was shifted downfield and changed into a singlet, and resonances for C-1 and C-15 were down-shifted by 37.1 and 8.4 ppm, respectively, in comparison with 13,14-dihydroxy-3,4-anhydrofloridanolide. This suggested that **8** was the 1-hydroxy derivative of 13,14-dihydroxy-3,4-anhydro-floridanolide. The

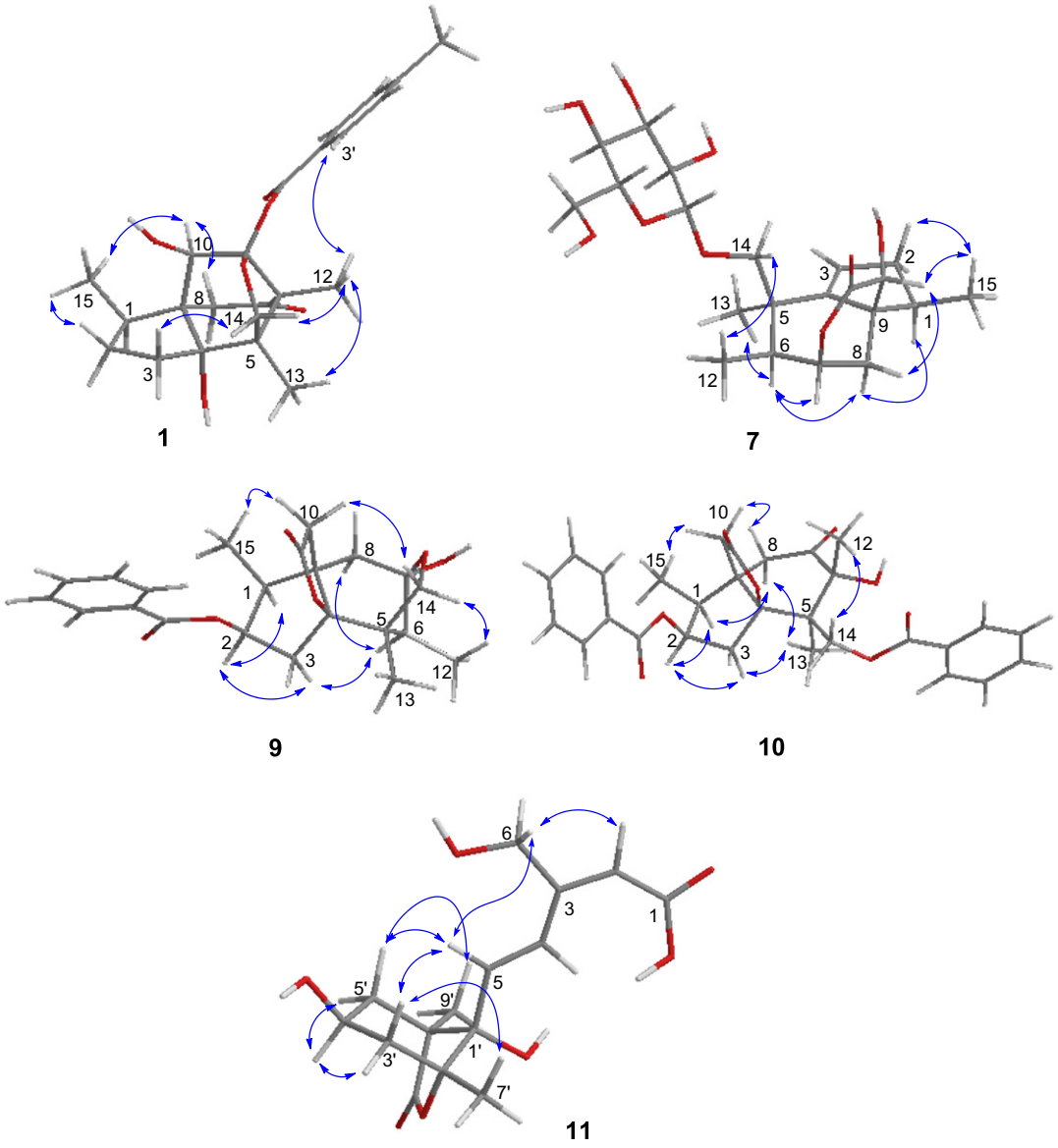

Fig. 3. Key NOESY correlations of **1**, **7**, **9**, **10**, and **11**.

relative configuration of **8** was identical with that of **7** and 13,14-dihydroxy-3,4-anhydrofloridanolide according to NOESY correlations. Consequently, **8** was established as 1,13,14-trihydroxy-3,4-anhydrofloridanolide, and named dunnianolide B (**8**).

Compound **9** was isolated as colorless needles, and its molecular formula $C_{22}H_{26}O_6$ was determined by positive HRESIMS (*m*/*z* 387.1804 $[M+H]^+$). Its IR spectrum displayed absorptions ascribable to hydroxy (3423 cm^{-1}), carbonyl (1747 and 1716 cm^{-1}), and phenyl (1601, 1585, and 1451 cm^{-1}) groups. The ^1H and ^{13}C NMR spectroscopic data (Tables 1 and 3) showed the presence of a benzoyl group [δ_H 8.00 (2H, d, J = 7.5 Hz, H-3′, 7′), 7.44 (2H, t, J = 7.5 Hz, H-4′, 6′), and 7.55 (1H, t, J = 7.5 Hz, H-5′); δ_C 166.2 (C-1′)]. Except for the benzoyl group, the ^{13}C NMR spectrum showed another 15 carbon signals, which were categorized by DEPT experiment as three methyls (CH_3-12, CH_3-13, CH_3-15), four methylenes including an oxygenated methylene (CH_2-3, CH_2-8, CH_2-10, and *O*-CH_2-14), three methines including an oxygenated methine (CH-1, *O*-CH-2, and CH-6), and five quaternary carbons including a carbonyl carbon at δ_C 176.1 (C-11) and a hemiketal-type carbon at δ_C 106.1 (C-7). The above features indicated that **9** was closely similar to pseudomajucin (Kouno et al., 1989b), except for the presence of an additional benzoyl group. By comparing the ^1H and ^{13}C NMR spectroscopic data of **9** with those of pseudomajucin, it was found that signals at δ_H 4.42 (H-2) and δ_C 73.6 (C-2) in pseudomajucin were shifted downfield to δ_H 5.52 (H-2) and δ_C 76.8 (C-2) in **9**, respectively, which indicated that the hydroxy group at C-2 in pseudomajucin was substituted by a benzoyloxy group in **9**. This was further confirmed by an HMBC correlation (Fig. 2) between H-2 (δ_H 5.52) and the carbonyl carbon at δ_C 166.2 (C-1′). The relative configuration of **9** was deduced from a NOESY experiment (Fig. 3). The NOESY spectrum showed cross-peaks between H-2 and both of H-1 and H-3α, and between H_3-15 and H-10a, which indicated that the benzoyloxy group and Me-15 were β-oriented. The correlations of H_3-12 to H-14b, of H-6 to H-3α and H-8α, and of H-14a to H-10b confirmed the β-orientation of Me-12 and the α-orientation of Me-13. Accordingly, **9** was elucidated as 2β-benzoyloxy-pseudomajucin, and designated as dunnianolide C (**9**).

Compound **10** was obtained as a colorless amorphous solid. Its molecular formula was established as $C_{29}H_{30}O_8$ by positive HRESIMS (*m*/*z* 529.1820 $[M+Na]^+$). Its IR spectrum showed absorptions

Table 3
^{1}H NMR spectroscopic data for compounds **7**–**10** (500 MHz, *J* in Hz).[a].

Position	7	8	9	10
1	2.04, m		2.29, m	2.36, m
2	Hα 2.28, ddd (14.0, 7.0, 3.0) Hβ 2.08, ddd (14.0, 9.5, 1.5)	Hα 2.25, dd (16.5, 1.5) Hβ 2.56, d (16.5)	5.52, br d (4.0)	5.57, br d (5.0)
3	5.94, dd (3.0, 1.5)	5.81, br s	Hα 2.31, dd (15.5, 4.5) Hβ 2.47, d (15.5)	Hα 3.13, dd (16.0, 6.0) Hβ 2.46, d (16.0)
6	1.77, qd (7.0, 2.5)		1.84, q (7.0)	
7	4.47, m	4.17, br s		
8α	1.62, dd (13.5, 1.5)	2.66, d (14.0)	1.90, d (14.0)	2.78, d (15.5)
8β	2.34, dd (13.5, 4.5)	1.70, dd (14.0, 3.5)	2.36, d (14.0)	2.89, d (15.5)
10	4.06, d (8.0)	4.09, s	Ha 3.00, d (18.5) Hb 2.90, d (18.5)	Ha 3.24, d (19.0) Hb 2.40, d (19.0)
12	1.13, d (7.0)	1.32, s	1.08, d (7.0)	1.46, s
13	1.25, s	3.25, s	1.06, s	1.24, s
14	Ha 3.70, d (9.5) Hb 3.33, d (9.5)	3.91, s	Ha 3.92, d (9.5) Hb 3.69, d (9.5)	Ha 4.68, d (12.0) Hb 4.58, d (12.0)
15	1.13, d (7.0)	1.28, s	1.08, d (7.0)	1.09, d (7.0)
1′	4.21, d (8.0)			
2′	3.22, (overlap)			
3′	3.31, (overlap)		8.00, d (7.5)	7.96, d (7.5)
4′	3.30, (overlap)		7.44, t (7.5)	7.45, t (7.5)
5′	3.24, (overlap)		7.55, t (7.5)	7.56, t (7.5)
6′	Ha 3.79, ddd (11.5, 6.0, 2.0) Hb 3.63, dd (11.5, 6.0)		7.44, t (7.5)	7.45, t (7.5)
7′			8.00, d (7.5)	7.96, d (7.5)
3″, 7″				7.96, d (7.5)
4″, 6″				7.47, t (7.5)
5″				7.58, t (7.5)
10-OH	3.97, d (8.0)			
2′-OH	3.89, d (3.5)			
3′-OH	4.11, (overlap)			
4′-OH	4.11, (overlap)			
6′-OH	3.58, dd (11.5, 6.0)			

[a] Measured in acetone-d_6 for compound **7**, in methanol-d_4 for compound **8**, and in $CDCl_3$ for compounds **9** and **10**.

ascribable to hydroxy (3361 cm^{-1}), γ-lactone (1773 cm^{-1}), carbonyl (1719 cm^{-1}), and phenyl (1601, 1584, and 1451 cm^{-1}) groups. Two benzoyl groups were readily observed in the ^{1}H and ^{13}C NMR spectroscopic data (Tables 1 and 3). In addition, the ^{1}H and ^{13}C NMR spectra showed the presence of two tertiary methyls [δ_H 1.24 (3H, s, H_3-13); 1.46 (3H, s, H_3-12)], a secondary methyl [δ_H 1.09 (3H, d, J = 7.0 Hz, H_3-15)], two isolated methylenes [δ_H 2.78 and 2.89 (each d, J = 15.5 Hz, H-8); δ_H 3.24 and 2.40 (each d, J = 19.0 Hz, H-10)], an oxygen-bearing isolated methylene [δ_H 4.68 and 4.58 (each d, J = 12.0 Hz, H-14)], and two carbonyl carbons at δ_C 174.4 (C-11) and δ_C 209.5 (C-7). The NMR spectroscopic data of **10** closely resembled those of (6*R*)-pseudomajucinone (Huang et al., 2002). However, it was observed that signals for H-2, H-14a, and H-14b were shifted downfield from δ_H 4.12, 3.62, and 3.53 in (6*R*)-pseudomajucinone to δ_H 5.57, 4.68, and 4.58 in **10**, respectively. This indicated that two benzoyl groups were esterified at C-2 and C-14, respectively, which were further confirmed by HMBC correlations (Fig. 2) between H-2 (δ_H 5.57) and the carbonyl carbon at δ_C 166.2 (C-1′) and between H-14a (δ_H 4.68) and C-1″ (δ_C 166.0). Moreover, the signal for H_3-12 (δ_H 1.46) changed to a singlet and resonance for C-6 in **10** was shifted downfield by 30.9 ppm, in comparison with (6*R*)-pseudomajucinone, which suggested that the proton at C-6 in (6*R*)-pseudomajucinone was replaced by a hydroxy group in **10**.

In addition, the relative configuration of **10** was elucidated by analysis of NOESY spectrum. NOESY correlations (Fig. 3) between H-2 and both of H-1 and H-3α, and between H_3-15 and H-10a suggested that 2-benzoyloxy group and Me-15 were β-oriented. The interactions between H_3-12 and H-14b, and between H_3-13 and both of H-3α and H-8α reflected the β-orientation of Me-12 and the α-orientation of Me-13. The absolute configuration of **10** was determined by analysis of its CD spectrum. On the basis of the octant rule for cyclohexanone (Kirk, 1986), the negative Cotton effect at 302 nm for the $n \rightarrow \pi^*$ transition indicated that the absolute configuration of **10** was (1*S*, 2*R*, 4*S*, 5*R*, 6*R*, 9*R*) (Fig. 4), consistent with the core configuration of (6*R*)-pseudomajucinone (Huang et al., 2002), whose absolute configuration have been established by X-ray crystallographic analysis. Therefore, **10** was determined to be (1*S*, 2*R*, 4*S*, 5*R*, 6*R*, 9*R*)-2,14-dibenzoyloxy-6-hydroxy-pseudomajucinone, and named dunnianolide D (**10**).

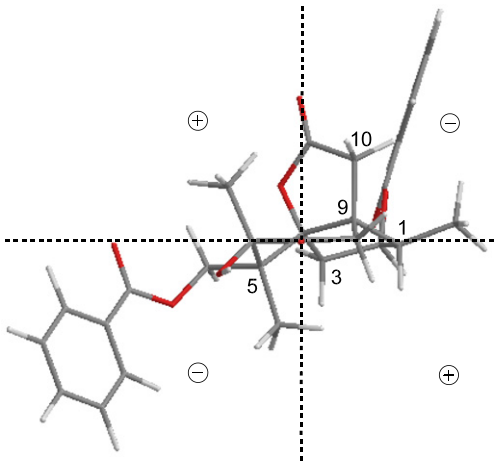

Fig. 4. Octant projection of **10**.

Compound **11** was isolated as colorless granules with the molecular formula of $C_{15}H_{20}O_7$ determined by positive HRESIMS (*m*/*z* 335.1099 $[M+Na]^+$). The characteristic absorption bands of hydroxy (3313 cm^{-1}), carbonyl (1763 cm^{-1}), conjugated carbonyl (1687

Table 4
^{13}C and ^{1}H NMR spectroscopic data for compounds **11** and **12**[a].

Position	**11**				**12**	
	δ_C[b]	δ_H (J in Hz) [b]	δ_C [c]	δ_H (J in Hz) [c]	δ_C [c]	δ_H (J in Hz) [c]
1	169.7		167.5		167.6	
2	117.9	6.10, s	116.5	6.15, s	115.2	6.11, s
3	153.0		153.3		153.9	
4	130.6	7.83, d (16.5)	129.7	7.89, d (16.5)	128.3	7.89, d (16.5)
5	130.9	6.42, d (16.5)	130.9	6.54, d (16.5)	133.6	6.55, d (16.5)
6	63.0	4.43, s	62.4	4.50, s	62.4	4.48, s
1′	82.8		82.5		83.0	
2′	89.8		88.2		86.7	
3′	42.2	H_{ax} 1.84, dd (14.0, 10.0) H_{eq} 2.26, dd (14.0, 7.0)	42.6	H_{ax} 1.91, dd (14.0, 10.0) H_{eq} 2.25, dd (14.0, 6.5)	46.5	H_{ax} 1.76, dd (13.5, 10.0) H_{eq} 1.99, dd (13.5, 7.0)
4′	65.2	H_{ax} 3.84, m	64.8	H_{ax} 3.87, m	65.4	H_{ax} 4.10, m
5′	40.9	H_{ax} 1.71, dd (13.5, 11.0) H_{eq} 1.90, dd (13.5, 7.0)	41.1	H_{ax} 1.79, dd (13.5, 11.0) H_{eq} 1.88, dd (13.5, 7.0)	45.0	H_{ax} 1.69, dd (13.5, 10.0) H_{eq} 1.83, dd (13.5, 7.0)
6′	53.5		52.8		49.2	
7′	18.4	1.34, s	18.5	1.35, s	19.9	1.09, s
8′	181.0		178.6		76.8	Ha 3.77, dd (7.0, 1.5) Hb 3.66, d (7.0)
9′	14.5	1.08, s	14.6	1.08, s	16.5	0.91, s

[a] Measured at 500 MHz for proton and 125 MHz for carbon.
[b] Measured in methanol-d_4.
[c] Measured in acetone-d_6.

cm^{-1}), and olefinic (1641 and 1603 cm^{-1}) groups were observed in the IR spectrum. The ^{1}H NMR spectrum of **11** (Table 4) showed signals for two tertiary methyls [δ_H 1.08 (3H, s, H_3-9′), δ_H 1.35 (3H, s, H_3-7′)], three methylenes including an oxygen-bearing isolated methylene [δ_H 1.91 (1H, dd, J = 14.0, 10.0 Hz, H-3′ax) and 2.25 (1H, dd, J = 14.0, 6.5 Hz, H-3′eq); δ_H 1.79 (1H, dd, J = 13.5, 11.0 Hz, H-5′ax) and 1.88 (1H, dd, J = 13.5, 7.0 Hz, H-5′eq); δ_H 4.50 (2H, s, H_2-6)], an oxymethine [δ_H 3.87 (1H, m, H-4′)], and three olefinic protons [δ_H 6.15 (1H, s, H-2), 6.54 (1H, d, J = 16.5 Hz, H-5), and 7.89 (1H, d, J = 16.5 Hz, H-4)]. The ^{13}C NMR and DEPT spectra displayed six nonprotonated carbons including an olefinic (δ_C 153.3, C-3), two carbonyl (δ_C 167.5, C-1 and 178.6, C-8′), a quaternary (δ_C 52.8, C-6′), and two oxygenated quaternary (δ_C 82.5, C-1′ and 88.2, C-2′) carbons together with nine protonated carbons. The ^{1}H–^{1}H COSY spectrum established the sequence of CH_2(3′)–CH(O)(4′)–CH_2(5′) and an olefin moiety (Fig. 2). The large vicinal coupling constant (16.5 Hz) between H-4 (δ_H 7.89) and H-5 (δ_H 6.54) suggested that the olefin moiety was in the *E* configuration. According to the above features, the NMR spectroscopic data (CD_3OD) of **11** were very similar to those of *rel*-5-(3*S*,8*S*-dihydroxy-1*R*,5*S*-dimethyl-7-oxa-6-oxobicyclo[3,2,1]oct-8-yl)-3-methyl-2*Z*,4*E*-pentadienoic acid (Kikuzaki et al., 2004), a derivative of dihydrophaseic acid (Milborrow, 1975), except for the absence of a signal for a tertiary methyl group and the presence of resonance for an oxygen-bearing isolated methylene group [δ_H 4.50 (2H, s, H_2-6)], which indicated that a proton of the methyl group at C-3 in *rel*-5-(3*S*,8*S*-dihydroxy-1*R*,5*S*-dimethyl-7-oxa-6-oxobicyclo[3,2,1]oct-8-yl)-3-methyl-2*Z*,4*E*-pentadienoic acid was replaced by a hydroxy group in **11**. This was further confirmed by HMBC correlations between the hydroxymethyl protons at δ_H 4.50 (H_2-6) and the olefinic carbons at δ_C 116.5 (C-2), 153.3 (C-3), and 129.7 (C-4) (Fig. 2).

The relative configuration of **11** was deduced from a NOESY experiment, in which the correlations between H_2-6 and both H-2 and H-5 verified the conjugated diene was 2*E*,4*E*-configuration. The cross-peaks between H-3′ax and both H_3-7′ and H-5, between H-5′ax and both H_3-9′ and H-5, and between H-4′ and both H-3′eq and H-5′eq were observed to establish the relative configuration as shown in Fig. 3. Thus, **11** was elucidated as 8′-oxo-6-hydroxy-dihydrophaseic acid (**11**).

Compound **12** was assigned the molecular formula $C_{15}H_{22}O_6$ obtained from positive HRESIMS (*m*/*z* 321.1307 $[M+Na]^+$). Its NMR spectroscopic data (Table 4) very resembled those of **11**. Comparing the ^{1}H and ^{13}C NMR spectra of **11**, the signals due to an isolated oxymethylene group were observed at δ_H 3.77 (1H, dd, J = 7.0, 1.5 Hz, H-8′a) and 3.66 (1H, d, J = 7.0 Hz, H-8′b) in the ^{1}H NMR and at δ_C 76.8 in the ^{13}C NMR spectra of **12**, with the disappearance of the carbonyl carbon at δ_C 178.6 assignable to C-8′ in **11**. In the HMBC spectrum of **12**, the oxymethylene proton at δ_H 3.66 (H-8′b) was correlated with C-1′ (δ_C 83.0), C-2′ (δ_C 86.7), C-5′ (δ_C 45.0), and C-6′ (δ_C 49.2), indicating that C-8′ was an oxymethylene carbon. The NOESY correlation between H-8′b (δ_H 3.66) and H-4′ax (δ_H 4.10) confirmed that the orientation of the oxymethylene was axial. Thus, **12** was determined to be 6-hydroxy-dihydrophaseic acid (**12**).

Compounds **1**–**16** were assessed for their inhibitory activities against the release of β-glucuronidase in rat PMNs induced by PAF *in vitro*. Ginkgolide B was used as a positive control (IC_{50} 2.92 ± 0.49 μM). Meanwhile, the tested compounds were not cytotoxic against rat PMNs in the MTT assay at a concentration of 10^{-5} M (See Supplementary data). As shown in Table 5, compounds **11** and **13** exhibited significant inhibitory activities, with IC_{50} values of 2.10 ± 0.40 and 1.93 ± 0.57 μM, respectively. Compounds **1**–**3**, **8**, **9**, **15**, and **16** showed moderate activities with the inhibitory rates ranging from 32.4 ± 1.4% to 43.4 ± 3.3% at a concentration of 10^{-5} M, while compounds **4**–**7** exhibited weak activities with the inhibitory rates ranging from 19.4 ± 2.7% to 28.6 ± 3.5% at the same concentration, and the other compounds were inactive. Primary discussion of structure–activity relationship revealed that for *allo*-cedrane sesquiterpenes, the benzoyloxy group at C-11 in **13** could significantly increase the activity in relative to the *p*-methyl benzoyloxy group in **1**, the *O*-cinnamoyl group in **2**, and the 11-*O*-2-methylcyclopent-1-enecarboxyl moiety in **14**, while the C-2 hydroxy group in **3** and the C-2 acetoxy group in **4** cause a drastic decrease in activity comparing with **13**. Thus, the occurrence of a benzoyloxy group at C-11 in addition to the lack of a hydroxy or acetoxy group at C-2 may be structural prerequisites for the activities against the release of β-glucuronidase in rat PMNs induced by PAF. In addition, the 8′-carbonyl group in **11** maybe involved in the activity.

Cytotoxic activities of compounds **1**–**16** were evaluated against five human cancer cell lines (A549, Bel-7402, BGC-823, HCT-8, and A2780) in the MTT assay, with adriamycin as a positive control

Table 5
Potency of compounds **1**–**16** in inhibiting the release of β-glucuronidase in rat PMNs induced by PAF[a].

Compound	IC_{50} (μM)	Inhibition rate (%)[b]
1	>10	40.4 ± 3.3
2	>10	35.8 ± 2.6
3	>10	32.4 ± 1.4
4	>10	20.3 ± 2.0
5	>10	26.6 ± 3.3
6	>10	19.4 ± 2.7
7	>10	28.6 ± 3.5
8	>10	40.9 ± 1.6
9	>10	33.4 ± 2.0
10	>10	−5.3 ± 5.2
11	2.10 ± 0.40	65.8 ± 3.0
12	>10	−34.5 ± 4.6
13	1.93 ± 0.57	65.0 ± 4.1
14	>10	−6.5 ± 3.2
15	>10	43.4 ± 3.3
16	>10	34.5 ± 2.8
Ginkgolide B[c]	2.92 ± 0.49	58.7 ± 1.6

[a] Data are mean ± standard deviation (n = 3).
[b] Inhibition rate (%) at 10 μM.
[c] Positive control.

(IC_{50} 0.23 ± 0.16, 0.53 ± 0.04, 0.97 ± 0.92, 0.61 ± 0.25, 0.63 ± 0.27 μM, respectively). None of them exhibited significant activities in the concentration range of 10^{-5}–10^{-7} M.

Some of the sesquiterpene lactones isolated from the genus *Illicium* were considered as responsible for the neurotoxicity of these plants (Kouno et al., 1989a; Yang et al., 1990, 1991). Such as anisatin with a β-lactone structure acts as a picrotoxin-like, non-competitive GABA antagonist (Kudo et al., 1981; Matsumoto and Fukuda, 1982). However, some sesquiterpenes have been found not to be neurotoxic, but to show neurotrophic activities (Fukuyama and Huang, 2005; Fukuyama et al., 2001, 1993; Huang et al., 2001a,c; Kubo et al., 2009; Yokoyama et al., 2002). These properties influence the application of the active sesquiterpene lactones as potential anti-inflammatory agents. Further studies are necessary to clarify the toxicological activities of these compounds.

3. Concluding remarks

Twelve new sesquiterpenes including six *allo*-cedrane sesquiterpenes (**1**–**6**), four *seco*-prezizaane-type sesquiterpenes (**7**–**10**), and two monocyclofarnesane sesquiterpenes (**11** and **12**), were isolated from the roots of *I. dunnianum* along with four known sesquiterpenes (**13**–**16**). *allo*-cedrane sesquiterpenes **1**–**6** possesses a rare oxatetracyclic system with a cagelike ketal structure, corresponding to a key precursor in the biogenesis of *seco*-prezizaane-type sesquiterpenes (Fukuyama et al., 1995; Schmidt et al., 2001). The discovery of compounds **1**–**6** is a further addition to the diversity of *allo*-cedrane sesquiterpenes. In addition, the activities against the release of β-glucuronidase in rat PMNs induced by PAF and cytotoxicities of the isolated compounds were also investigated.

4. Experimental

4.1. General experimental procedures

Melting points were measured on a XT-5B micromelting point apparatus and were uncorrected. Optical rotations were taken on a JASCO P-2000 automatic digital polarimeter. UV spectra were measured on a JASCO V650 spectrophotometer. CD spectra were measured on a JASCO J-815 spectrometer. IR spectra were recorded on a Nicolet 5700 FT-IR spectrometer. NMR spectra were recorded on an INOVA-500 spectrometer at 25 °C. ESIMS was measured on an Agilent 1100 Series LC/MSD ion trap mass spectrometer. HRESIMS data were recorded on an Agilent Technologies 6250 Accurate-Mass Q-TOF LC/MS spectrometer. Analytical HPLC was performed on an Agilent 1100 Series instrument with a DAD detector, using a YMC-Pack ODS (250 × 4.6 mm, 5 μm). Preparative HPLC was performed on a Shimadzu LC-6AD instrument with an SPD-10A detector, using a YMC-Pack ODS-A column (250 × 20 mm, 5 μm). GC data were recorded on an Agilent 7890A instrument with an FID detector. Sephadex LH-20 (Amersham Pharmacia Biotech AB, Sweden), ODS (45–70 μm, Merck), silica gel (160–200, 200–300 mesh, Qingdao Marine Chemical Co. Ltd., China), and diatomite (Sinopharm Chemical Reagent Co. Ltd., China) were used for column chromatography (CC). TLC was carried out with glass precoated with silica gel GF_{254} plates (Qingdao Marine Chemical Co. Ltd., China). Spots were visualized under UV light or by spraying with 10% H_2SO_4 in EtOH–H_2O (95:5, v/v) followed by heating. Solvents [petroleum ether (60–90 °C), $CHCl_3$, EtOAc, MeOH, CH_2Cl_2, and EtOH] were of analytical grade and purchased from Beijing Chemical Company, Beijing, China.

4.2. Plant material

Roots of *I. dunnianum* were collected in Guangxi Province, China, in November 2009, and identified by Prof. Song-Ji Wei of Guang Xi College of Traditional Chinese Medicine. A voucher specimen (No. ID-S-2328) was deposited in the herbarium of the Department of Medicinal plants, Institute of Materia Medica, Chinese Academy of Medical Sciences.

4.3. Extraction and isolation

Roots of *I. dunnianum* (7.5 kg) were air-dried, ground, and extracted three times (2 h for each time) with EtOH–H_2O (3 × 80 l, 95:5, v/v) under conditions of reflux (90–95 °C), and the residue was refluxed with EtOH–H_2O (2 × 64 l, 70:30, v/v). The combined EtOH extract was evaporated to near dryness under reduced pressure to give the crude extract (850 g), which was absorbed by diatomite, and then successively extracted with petroleum ether (60–90 °C) (10 l), $CHCl_3$ (10 l), EtOAc (10 l), and MeOH (10 l). The $CHCl_3$ extract (49 g) was subjected to a silica gel CC (40 × 7 cm, 160–200 mesh), eluted with CH_2Cl_2–MeOH (100:1, 50:1, 20:1, 10:1, 5:1, 2:1, v/v) to yield nine fractions C1–C9 on the basis of TLC analysis. Fraction C4 (8.0 g) was subjected to a ODS CC, eluted with a gradient of MeOH–H_2O (10:90 → 100:0) to give fractions C4-1–C4-20. Fraction C4-5 (102 mg) was purified by preparative HPLC using CH_3CN–H_2O (20:80, 8 ml/min) to yield compound **16** (54.0 mg, t_R 36 min, purity 97.1%). Fraction C4-6 (122 mg) was separated by preparative HPLC using CH_3CN–H_2O (40:60, 8 ml/min) to afford compounds **9** (42.0 mg, t_R 33 min, purity 97.4%) and **15** (25.2 mg, t_R 40 min, purity 97.7%). Fraction C4-8 (65 mg) was separated by preparative HPLC using CH_3CN–H_2O (50:50, 8 ml/min) to yield compound **4** (9.3 mg, t_R 29 min, purity 92.4%). Fraction C4-10 (250 mg) was applied to preparative HPLC using CH_3CN–H_2O (50:50, 7 ml/min) to yield compound **14** (112.0 mg, t_R 41 min, purity 96.3%). Fraction C4-11 (60 mg) was separated by preparative HPLC using CH_3CN–H_2O (48:52, 8 ml/min) to yield compound **6** (21.0 mg, t_R 39 min, purity 96.9%). Fraction C4-12 (0.5 g) was subjected to Sephadex LH-20 CC eluted with CH_2Cl_2–MeOH (1:2) and then further purified by preparative HPLC using CH_3CN–H_2O (60:40, 7 ml/min) to yield compounds **1** (3.0 mg, t_R 36 min, purity 91.8%), **2** (6.1 mg, t_R 34 min, purity 93.8%), **10** (3.1 mg, t_R 30 min, purity 96.3%), and **13** (156.0 mg, t_R 38 min, purity 99.2%). Fraction C6 (3.8 g) was applied to an ODS CC eluted with a gradient of MeOH–H_2O (10:90 → 90:10) to give nine fractions C6-1–C6-9. Fraction C6-2 (215 mg) and C6-3 (280 mg) were subjected to Sephadex LH-20 CC eluted with MeOH and then further purified by preparative HPLC using CH_3CN–H_2O (41:59, 7 ml/min) and (45:55, 7 ml/min),

to yield compounds **3** (27.1 mg, t_R 24 min, purity 98.0%) and **5** (46.0 mg, t_R 22 min, purity 99.0%), respectively.

The EtOAc extract (110 g) was subjected to a silica gel CC (50 × 8 cm, 160–200 mesh) eluted with $CHCl_3$–MeOH (50:1, 20:1, 10:1, 5:1, 1:1, 0:1, v/v) to afford nine fractions E1–E9. Fraction E4 (4.5 g) was applied to an ODS CC eluted with a gradient of MeOH–H_2O (10:90 → 100:0) to yield nine fractions E4-1–E4-9. Fraction E4-3 (160 mg) was submitted to a Sephadex LH-20 CC eluted with MeOH, then purified by preparative HPLC using 0.1% TFA in CH_3CN–H_2O (12:88, 7 ml/min) to afford compound **11** (27.1 mg, t_R 20 min, purity 96.2%). Fraction E4-5 (150 mg) was separated by preparative HPLC using CH_3CN–H_2O (28:72, 7 ml/min) to yield compound **7** (20.0 mg, t_R 22 min, purity 96.7%). Fraction E5 (8.4 g) was subjected to an ODS CC eluted with a gradient of MeOH–H_2O (10:90 → 100:0) to give 18 fractions E5-1–E5-18. Fraction E5-4 (70 mg) was separated by preparative HPLC using 0.1% TFA in CH_3CN–H_2O (5:95, 7 ml/min) to yield compound **8** (9.0 mg, t_R 30 min, purity 92.1%). Fraction E5-6 (125 mg) was subjected to a Sephadex LH-20 CC eluted with MeOH, and further purified by preparative HPLC using 0.1% TFA in CH_3CN/H_2O (11:89, 7 ml/min) to yield compound **12** (5.1 mg, t_R 17 min, purity 95.2%). (The purity of isolated compounds was determined by HPLC).

4.3.1. Tashironin B (**1**)

Colorless amorphous solid; $[\alpha]_D^{20}$–15.7 (*c* 0.1, MeOH); UV (MeOH) λ_{max} (logε) 204 (3.81), 241 (3.79), 274 (2.80) nm; IR (KBr) ν_{max} 3485, 2951, 2911, 1713, 1612, 1458, 1416, 1386, 1284, 1030, 751 cm^{-1}; For ^{13}C and ^{1}H NMR spectroscopic data, see Tables 1 and 2; ESIMS *m/z* 401 $[M+H]^+$, 423 $[M+Na]^+$, 439 $[M+K]^+$, 399 $[M-H]^-$, 435 $[M+Cl]^-$; HRESIMS *m/z* 423.1784 $[M+Na]^+$ (calcd. for $C_{23}H_{28}O_6Na$, 423.1778).

4.3.2. Tashironin C (**2**)

Colorless amorphous solid; $[\alpha]_D^{20}$–43.3 (*c* 0.03, MeOH); UV (MeOH) λ_{max} (logε) 206 (4.11), 218 (4.16), 283 (4.33) nm; IR (KBr) ν_{max} 3445, 2944, 1712, 1635, 1450, 1386, 1334, 1284, 1173, 1027, 769 cm^{-1}; For ^{13}C and ^{1}H NMR spectroscopic data, see Tables 1 and 2; ESIMS *m/z* 435 $[M+Na]^+$, 451 $[M+K]^+$, 131 $[C_8H_7CO]^+$, 411 $[M-H]^-$, 447 $[M+Cl]^-$; HRESIMS *m/z* 435.1788 $[M+Na]^+$ (calcd. for $C_{24}H_{28}O_6Na$, 435.1778).

4.3.3. 2α-Hydroxytashironin (**3**)

Colorless amorphous solid; $[\alpha]_D^{20}$–19.1 (*c* 0.1, MeOH); UV (MeOH) λ_{max} (logε) 201 (4.30), 233 (4.17), 276 (3.14) nm; IR (KBr) ν_{max} 3516, 2973, 2934, 1720, 1600, 1493, 1452, 1391, 1278, 1024, 712 cm^{-1}; For ^{13}C and ^{1}H NMR spectroscopic data, see Tables 1 and 2; ESIMS *m/z* 403 $[M+H]^+$, 425 $[M+Na]^+$, 441 $[M+K]^+$, 437 $[M+Cl]^-$; HRESIMS *m/z* 425.1587 $[M+Na]^+$ (calcd. for $C_{22}H_{26}O_7Na$, 425.1571).

4.3.4. 2α-Acetoxytashironin (**4**)

Colorless amorphous solid; $[\alpha]_D^{20}$+4.4 (*c* 0.09, MeOH); UV (MeOH) λ_{max} (logε) 203 (3.21), 232 (3.41), 275 (2.38) nm; IR (KBr) ν_{max} 3438, 2963, 2927, 1720, 1638, 1275, 1024, 713 cm^{-1}; For ^{13}C and ^{1}H NMR spectroscopic data, see Tables 1 and 2; ESIMS *m/z* 467 $[M+Na]^+$, 483 $[M+K]^+$, 443 $[M-H]^-$, 479$[M+Cl]^-$; HRESIMS *m/z* 467.1687 $[M+Na]^+$ (calcd. for $C_{24}H_{28}O_8Na$, 467.1676).

4.3.5. 2α-Hydroxytashironin A (**5**)

Colorless granules (EtOAc); mp 144–145 °C; $[\alpha]_D^{20}$–13.6 (*c* 0.1, MeOH); UV (MeOH) λ_{max} (logε) 198 (3.81), 238 (4.14) nm; IR (KBr) ν_{max} 3510, 2950, 2908, 1708, 1641, 1260, 1111, 1067, 1029, 767 cm^{-1}; For ^{13}C and ^{1}H NMR spectroscopic data, see Tables 1 and 2; ESIMS *m/z* 407 $[M+H]^+$, 429 $[M+Na]^+$, 445 $[M+K]^+$, 405 $[M-H]^-$, 441 $[M+Cl]^-$; HRESIMS *m/z* 429.1861 $[M+Na]^+$ (calcd. for $C_{22}H_{30}O_7Na$, 429.1884).

4.3.6. 2α-Acetoxytashironin A (**6**)

Colorless needles (EtOAc); mp 154–155 °C; $[\alpha]_D^{20}$+6.3 (*c* 0.09, MeOH); UV (MeOH) λ_{max} (logε) 200 (3.69), 236 (3.84) nm; IR (KBr) ν_{max} 3516, 2973, 1728, 1712, 1641, 1266, 1060, 1028, 879 cm^{-1}; For ^{13}C and ^{1}H NMR spectroscopic data, see Tables 1 and 2; ESIMS *m/z* 471 $[M+Na]^+$, 487 $[M+K]^+$, 447 $[M-H]^-$, 483 $[M+Cl]^-$; HRESIMS *m/z* 471.1971 $[M+Na]^+$ (calcd. for $C_{24}H_{32}O_8Na$, 471.1989).

4.3.7. Dunnianolide A (**7**)

Colorless amorphous solid; $[\alpha]_D^{20}$+9.3 (*c* 0.06, MeOH); UV (MeOH) λ_{max} (logε) 202 (3.94), 233 (2.99), 280 (2.56) nm; IR (KBr) ν_{max} 3437, 2929, 1719, 1102, 1078, 1040, 756 cm^{-1}; For ^{13}C and ^{1}H NMR spectroscopic data, see Tables 1 and 3; ESIMS *m/z* 429 $[M+H]^+$, 451 $[M+Na]^+$, 467 $[M+K]^+$, 463 $[M+Cl]^-$; HRESIMS *m/z* 451.1939 $[M+Na]^+$ (calcd. for $C_{21}H_{32}O_9Na$, 451.1939).

4.3.8. Dunnianolide B (**8**)

Colorless amorphous solid; $[\alpha]_D^{20}$+70.2 (*c* 0.08, MeOH); UV (MeOH) λ_{max} (logε) 205 (3.50) nm; IR (KBr) ν_{max} 3331, 2934, 1725, 1677, 1205, 1086, 923, 763 cm^{-1}; For ^{13}C and ^{1}H NMR spectroscopic data, see Tables 1 and 3; ESIMS *m/z* 337 $[M+Na]^+$, 651 $[2M+Na]^+$, 427 $[M+CF_3COO]^-$; HRESIMS *m/z* 337.1261 $[M+Na]^+$ (calcd. for $C_{15}H_{22}O_7Na$, 337.1258).

4.3.9. Dunnianolide C (**9**)

Colorless needles (*n*-Hexane–EtOAc); mp 162–164 °C; $[\alpha]_D^{20}$–39.8 (*c* 0.06, MeOH); UV (MeOH) λ_{max} (logε) 201 (4.06), 230 (4.02), 274 (2.88) nm; IR (KBr) ν_{max} 3423, 2972, 2938, 2880, 1748, 1716, 1601, 1585, 1493, 1452, 1317, 1281, 1110, 1015, 714 cm^{-1}; For ^{13}C and ^{1}H NMR spectroscopic data, see Tables 1 and 3; ESIMS *m/z* 387 $[M+H]^+$, 409 $[M+Na]^+$, 425 $[M+K]^+$, 385 $[M-H]^-$, 421 $[M+Cl]^-$; HRESIMS *m/z* 387.1804 $[M+H]^+$ (calcd. for $C_{22}H_{27}O_6$, 387.1802).

4.3.10. Dunnianolide D (**10**)

Colorless amorphous solid; $[\alpha]_D^{20}$–37.8 (*c* 0.1, MeOH); CD (MeOH) λ_{max} ($\delta\varepsilon$) 280 (+0.19), 302 (−0.17); UV (MeOH) λ_{max} (logε) 203 (3.80), 229 (4.01), 274 (3.02) nm; IR (KBr) ν_{max} 3361, 2964, 2930, 1774, 1719, 1601, 1584, 1468, 1451, 1315, 1272, 1025, 713 cm^{-1}; For ^{13}C and ^{1}H NMR spectroscopic data, see Tables 1 and 3; ESIMS *m/z* 529 $[M+Na]^+$, 545 $[M+K]^+$, 505 $[M-H]^-$, 541 $[M+Cl]^-$; HRESIMS *m/z* 529.1820 $[M+Na]^+$ (calcd. for $C_{29}H_{30}O_8Na$, 529.1833).

4.3.11. 8′-Oxo-6-hydroxy-dihydrophaseic acid (**11**)

Colorless granules (*n*-hexane–EtOAc); mp 164–165 °C; [$[\alpha]_D^{20}$–65.3 (*c* 0.1, MeOH); UV (MeOH) λ_{max} (logε) 200 (3.81), 259 (4.18) nm; IR (KBr) ν_{max} 3313, 2974, 2937, 2895, 1763, 1688, 1641, 1603, 1382, 1243, 1050, 884 cm^{-1}; For ^{13}C and ^{1}H NMR spectroscopic data, see Table 4; ESIMS *m/z* 335 $[M+Na]^+$, 647 $[2M+Na]^+$, 623 $[2M-H]^-$; HRESIMS *m/z* 335.1099 $[M+Na]^+$ (calcd. for $C_{15}H_{20}O_7Na$, 335.1101).

4.3.12. 6-Hydroxy-dihydrophaseic acid (**12**)

Colorless needles (EtOAc); mp 104–106 °C; $[\alpha]_D^{20}$–10.9 (*c* 0.07, MeOH); UV (MeOH) λ_{max} (logε) 197 (3.86), 256 (4.18) nm; IR (KBr) ν_{max} 3465, 3368, 2937, 2884, 1686, 1642, 1610, 1421, 1379, 1248, 1234, 1037, 885 cm^{-1}; For ^{13}C and ^{1}H NMR spectroscopic data, see Table 4; ESIMS *m/z* 321 $[M+Na]^+$, 619 $[2M+Na]^+$, 297 $[M-H]^-$, 595 $[2M-H]^-$; HRESIMS *m/z* 321.1307 $[M+Na]^+$ (calcd. for $C_{15}H_{22}O_6Na$, 321.1309).

4.4. Acid hydrolysis and determination of the absolute configuration of the monosaccharide (Hara et al., 1987)

Compound **7** (8 mg) was hydrolyzed by 2 M HCl–H_2O (15 ml) at 95 °C for 10 h. The reaction mixture was diluted with H_2O and extracted with EtOAc (3 × 15 ml). The aqueous layer was evaporated to dryness under vacuum, diluted repeatedly with H_2O, and evaporated in vacuo to give a neutral monosaccharide residue. From the residue, glucose was detected by TLC [CH_2Cl_2:MeOH (5:1), *Rf* 0.43] with authentic sample. The residue (2 mg) was dissolved in pyridine (1 ml) containing L-cysteine methyl ester hydrochloride (2 mg) and heated at 60 °C for 2 h, then evaporated under N_2 stream and dried in vacuo. The residue was dissolved in *N*-trimethylsilylimidazole (0.2 ml) and heated at 60 °C for 2 h. The reaction mixture was partitioned between *n*-hexane and H_2O (2 ml each), and the *n*-hexane extract was analyzed by GC (Agilent 7890A) under the following conditions: capillary column HP-5 (30 m × 0.32 mm × 0.25 μm); detector FID; carrier gas N_2, flow rate 1 ml/min; detector temperature 280 °C; injection temperature 250 °C; oven temperature gradient: 100 °C for 2 min, 100 °C → 280 °C (10 °C/min), 280 °C for 5 min. The same procedure was applied to authentic sample. By comparison with retention time of authentic sample ($t_{R\text{-D-glucose}}$ 19.851 min), D-glucose ($t_{R\text{-}7}$ 19.850 min) was identified for compound **7**.

4.5. Activity assay against the release of β-glucuronidase (Kang et al., 2006)

Compounds **1**–**16** were assessed for their inhibitory activities against the release of β-glucuronidase in rat PMNs induced by PAF *in vitro*. Ginkgolide B (purity >90%; Sigma–Aldrich; St. Louis, MO, USA) was used as a positive control. Briefly, each test sample was dissolved in DMSO at a concentration of 0.1 M and diluted with RPMI-1640 to 10^{-3}–10^{-5} M. The test samples (2.5 μl) were incubated with a suspension of rat PMNs (245 μl) at a density of 2.5×10^6 cells ml^{-1} at 37 °C for 15 min, and 1×10^{-3} M cytochalasin B (2.5 μl) was added for another 5 min. After addition of PAF (2.5 μl), the mixture was incubated for another 5 min. Subsequently, the mixture was put in an ice-bath to terminate the reaction. After centrifugation at 1000 rpm for 5 min, the supernatant was obtained. The supernatant (25 μl) and 2.5 mM phenolphthaleinglucuronic acid (25 μl) were incubated with 0.1 M HOAc buffer (100 μl, pH 4.6) at 37 °C for 18 h. The reaction was terminated by the addition of 0.3 M NaOH (150 μl). The absorbance was read at 550 nm, and the inhibitory ratio (IR) was calculated as IR (%) = $(A_{PAF} - A_t)/(A_{PAF} - A_C) \times 100\%$, where A_{PAF}, A_t, and A_C refer to the average absorbance of three wells of PAF, test compounds, and control groups, respectively. The compounds (IR > 50% at 10 μM) were tested at three concentrations (0.1, 1, 10 μM) and each concentration of the compounds was tested in three parallel wells. A dose–response curve was plotted for each compound, and the IC_{50} value was calculated as the concentration of test compound resulting in 50% reduction of optical density compared with the control.

4.6. Cytotoxicity assay

The cytotoxicity assay against A549 (human lung epithelial cancer), Bel-7402 (human hepatoma cancer), BGC-823 (human gastric cancer), HCT-8 (human colon cancer), and A2780 (human ovarian cancer) cells was assessed using the MTT method as described in the literature (Alley et al., 1988). Adriamycin (purity >98%; Sigma–Aldrich; St. Louis, MO, USA) was used as a positive control.

Acknowledgments

This project was supported by the Natural Science Foundation of China (No. 201072234, No. 21132009), and the National Science and Technology Project of China (No. 2012ZX09301002-002). We are grateful to the Department of Instrumental Analysis, Institute of Materia Medica, Chinese Academy of Medical Sciences and Peking Union Medical College for measuring the IR, UV, NMR, and MS spectra.

Appendix A. Supplementary data

Supplementary data associated with this article can be found, in the online version, at http://dx.doi.org/10.1016/j.phytochem.2012.05.015.

References

Alley, M.C., Scudiero, D.A., Monks, A., Hursey, M.L., Czerwinski, M.J., Fine, D.L., Abbott, B.J., Mayo, J.G., Shoemaker, R.H., Boyd, M.R., 1988. Feasibility of drug screening with panels of human tumor cell lines using a microculture tetrazolium assay. Cancer Res. 48, 589–601.

Fukuyama, Y., Huang, J.M., 2005. Chemistry and neurotrophic activity of *seco*-prezizaane- and anislactone-type sesquiterpenes from *Illicium* species. Stud. Nat. Prod. Chem. 32, 395–427.

Fukuyama, Y., Huang, J.M., Nakade, K., Yokoyama, R., 2001. Structure and neurotrophic activity of anislactone-type sesquiterpenes from *Illicum merrillianum*. Tennen Yuki Kagobutsu Toronkai Koen Yoshishu 43, 425–430.

Fukuyama, Y., Shida, N., Kodama, M., 1993. Isodunnianin: a new sesquiterpene enhancing neurite outgrowth in primary culture of fetal rat cerebral hemisphere from *Illicium tashiroi*. Planta Med. 59, 181–182.

Fukuyama, Y., Shida, N., Kodama, M., 1995. Tashironin, a plausible biosynthetic precursor of anisatin-type sesquiterpenes. Tetrahedron Lett. 36, 583–586.

Hara, S., Okabe, H., Mihashi, K., 1987. Gas-liquid chromatographic separation of aldose enantiomers as trimethylsilyl ethers of methyl 2-(polyhydroxyalkyl)-thiazolidine-4(*R*)-carboxylates. Chem. Pharm. Bull. 35, 501–506.

Huang, J.M., Yokoyama, R., Yang, C.S., Fukuyama, Y., 2001a. Structure and neurotrophic activity of *seco*-prezizaane-type sesquiterpenes from *Illicium merrillianum*. J. Nat. Prod. 64, 428–431.

Huang, J.M., Yang, C.S., Takahashi, H., Fukuyama, Y., 2000a. *seco*-Prezizaane-type sesquiterpenes from *Illicium merrillianum*. Phytochemistry 55, 883–886.

Huang, J.M., Fukuyama, Y., Yang, C.S., Minami, H., Tanaka, M., 2000b. Three new sesquiterpene lactones from the pericarps of *Illicium merrillianum*. Chem. Pharm. Bull. 48, 657–659.

Huang, J.M., Yang, C.S., Kondo, M., Nakade, K., Takahashi, H., Takaoka, S., Fukuyama, Y., 2002. Merrillianin, a unique *seco*-prezizaane-type sesquiterpene, and (6*R*)-pseudomajucin from *Illicium merrillianum*. Tetrahedron 58, 6937–6941.

Huang, J.M., Yang, C.S., Tanaka, M., Fukuyama, Y., 2001b. Structures of merrilactones B and C, novel anislactone-type sesquiterpenes from *Illicium merrillianum*, and chemical conversion of anislactone B to merrilactone A. Tetrahedron 57, 4691–4698.

Huang, J.M., Yokoyama, R., Yang, C.S., Fukuyama, Y., 2000c. Merrilactone A, a novel neurotrophic sesquiterpene dilactone from *Illicium merrillianum*. Tetrahedron Lett. 41, 6111–6114.

Kang, J., Chen, R.Y., Yu, D.Q., 2006. Five new diels-alder type adducts from the stem and root bark of *Morus mongolica*. Planta Med. 72, 52–59.

Kikuzaki, H., Kayano, S.I., Fukutsuka, N., Aoki, A., Kasamatsu, K., Yamasaki, Y., Mitani, T., Nakatani, N., 2004. Abscisic acid related compounds and lignans in Prunes (*Prunus domestica* L.) and their oxygen radical absorbance capacity (ORAC). J. Agric. Food Chem. 52, 344–349.

Kirk, D.N., 1986. The chiroptical properties of carbonyl compounds. Tetrahedron 42, 777–818.

Kouno, I., Baba, N., Hashimoto, M., Kawano, N., Takahashi, M., Kaneto, H., Yang, C., Sato, S., 1989a. Isolation of three new sesquiterpene lactones from the pericarps of *Illicium majus*. Chem. Pharm. Bull. 37, 2448–2451.

Kouno, I., Baba, N., Hashimoto, M., Kawano, N., Yang, C., Sato, S., 1989b. A new sesquiterpene lactone and its glucoside from the pericarps of *Illicium majus*. Chem. Pharm. Bull. 37, 2427–2430.

Kouno, I., Mori, K., Kawano, N., Sato, S., 1989c. Structure of anislactone A; a new skeletal type of sesquiterpene from the pericarps of *Illicium anisatum*. Tetrahedron Lett. 30, 7451–7452.

Kubo, M., Okada, C., Huang, J.-M., Harada, K., Hioki, H., Fukuyama, Y., 2009. Novel pentacyclic *seco*-prezizaane-type sesquiterpenoids with neurotrophic properties from *Illicium jiadifengpi*. Org. Lett. 11, 5190–5193.

Kudo, Y., Oka, J., Yamada, K., 1981. Anisatin, a potent GABA antagonist, isolated from *Illicium anisatum*. Neurosci. Lett. 25, 83–88.

Ma, S.G., Tang, W.Z., Liu, Y.X., Hu, Y.C., Yu, S.S., Zhang, Y., Chen, X.G., Qu, J., Ren, J.H., Liu, Y.B., Xu, S., Liu, J., Liu, Y.Y., Li, Y., Lu, H.N., Wu, X.F., 2011. Prenylated C6–C3 compounds with molecular diversity from the roots of *Illicium oligandrum*. Phytochemistry 72, 115–125.

Matsumoto, K., Fukuda, H., 1982. Anisatin modulation of GABA- and pentobarbital-induced enhancement of diazepam binding in rat brain. Neurosci Lett.FIELD Full Journal Title:Neuroscience letters 32, 175–179.

Milborrow, B.V., 1975. The absolute configuration of phaseic and dihydrophaseic acids. Phytochemistry 14, 1045–1053.

Schmidt, T.J., 1999. Novel *seco*-prezizaane sesquiterpenes from North American *Illicium* species. J. Nat. Prod. 62, 684–687.

Schmidt, T.J., Mueller, E., Fronczek, F.R., 2001. New *allo*-cedrane type sesquiterpene hemiketals and further sesquiterpene lactones from fruits of *Illicium floridanum*. J. Nat. Prod. 64, 411–414.

Song, W.Y., Ma, Y.B., Bai, X., Zhang, X.M., Gu, Q., Zheng, Y.T., Zhou, J., Chen, J.J., 2007. Two new compounds and anti-HIV active constituents from *Illicium verum*. Planta Med. 73, 372–375.

Tang, W.Z., Liu, Y.B., Yu, S.S., Qu, J., Su, D.M., 2007. New sesquiterpene lactone and neolignan glycosides with antioxidant and anti-inflammatory activities from the fruits of *Illicium oligandrum*. Planta Med. 73, 484–490.

Tang, W.Z., Ma, S.G., Yu, S.S., Qu, J., Liu, Y.B., Liu, J., 2009. Rearranged prenylated C6–C3 compounds and a highly oxygenated *seco*-prezizaane-type sesquiterpene from the stem bark of *Illicium oligandrum*. J. Nat. Prod. 72, 1017–1021.

Yamada, K., Takada, S., Nakamura, S., Hirata, Y., 1968. Structures of anisatin and neoanisatin toxic sesquiterpenes from *Illicium anisatum*. Tetrahedron 24, 199–229.

Yang, C., Hashimoto, M., Baba, N., Takahshi, M., Kaneto, H., Kawano, N., Kouno, I., 1990. A new toxic neoanisatin derivative from the pericarps of *Illicium majus*. Chem. Pharm. Bull. 38, 291–292.

Yang, C.S., Wang, J.L., Zhang, Z.L., Kouno, I., 1991. Toxic constituents of *Illicium simonsii* Maxim. Yaoxue Xuebao 26, 128–131.

Yokoyama, R., Huang, J.M., Yang, C.S., Fukuyama, Y., 2002. New *seco*-prezizaane-type sesquiterpenes, jiadifenin with neurotrophic activity and 1,2-dehydroneomajucin from *Illicium jiadifengpi*. J. Nat. Prod. 65, 527–531.

Zhang, J., 1989. Chemical constituents of the stems and leaves of *Illicium dunnianum* Tutch. Zhongguo Zhongyao Zazhi 14, 36–37.